Supplemental information

The gonadal niche safeguards

human fetal germline cell development

following maternal SARS-CoV-2 infection

Shijun Shen, Mengting Wang, Xiaocui Li, Beiying Wang, Wei Hong, Wei Li, Ben Xu, Zhenxiang Guo, Ruichen Han, Shanru Yi, Zhiping Wu, Xiaoying He, Liping Wang, Qianshu Zhu, Guang Yang, Hong Wang, Qiaolin Deng, Jiayu Chen, Shaorong Gao, Cizhong Jiang, and Rui Gao

Document S1. Figure S1-S6, related to Figure 1-4.

Figure S1. Isolation of human FGCs and gonadal somatic cells by FACS following maternal SARS-CoV-2 infection, related to Figure 1.

Figure S2. Expression pattern of human FGCs following maternal SARS-CoV-2 infection, related to Figure 2, 3.

Figure S3. DNA methylation pattern of human FGCs and gonadal somatic cells following maternal SARS-CoV-2 infection, related to Figure 2, 3.

Figure S4. DNA methylation reprogramming faithfully maintained in human FGCs following maternal SARS-CoV-2 infection, related to Figure 3.

Figure S5. Extensive immune responses in gonadal niche shield FGCs from maternal SARS-CoV-2 infection, related to Figure 4.

Figure S6. Human FGC-niche communication was not compromised following maternal SARS-CoV-2 infection, related to Figure 4.

A

Patient ID	Maternal SARS-CoV-2 status	Gender	Gestational age at infection	Gestational age at termination	hFGC		Soma	
					Total RNA-seq	WGBS-seq	Total RNA-seq	WGBS-seq
P1	Maternal exposed (CoV)	Female	4W	11W	√		√	
P2	Maternal exposed (CoV)	Female	3W	11W	√		√	
P3	Maternal exposed (CoV)	Female	3W	11W	√		√	
P4	Maternal exposed (CoV)	Female	4D	12W	√		√	
P5	Maternal exposed (CoV)	Female	5W	13W	√		√	
P6	Maternal exposed (CoV)	Female	2W	13W	√	√	√	√
P7	Maternal exposed (CoV)	Female	5W	15W	√		√	
P8	Uninfected (Ctrl)	Female	N/A	11W	√		√	
P9	Uninfected (Ctrl)	Female	N/A	11W	√		√	
P10	Uninfected (Ctrl)	Female	N/A	12W	√		√	
P11	Uninfected (Ctrl)	Female	N/A	14W	√		√	
P12	Uninfected (Ctrl)	Female	N/A	16W	√		√	
P13	Maternal exposed (CoV)	Male	4W	10W	√		√	
P14	Maternal exposed (CoV)	Male	2W	11W	√		√	
P15	Maternal exposed (CoV)	Male	4W	11W	√		√	
P16	Maternal exposed (CoV)	Male	7W	11W	√		√	
P17	Maternal exposed (CoV)	Male	3W	12W	√	√	√	√
P18	Maternal exposed (CoV)	Male	2W	12W	√	√	√	√
P19	Maternal exposed (CoV)	Male	5W	13W	√		√	
P20	Maternal exposed (CoV)	Male	5W	14W	√		√	
P21	Maternal exposed (CoV)	Male	5W	15W	√		√	
P22	Maternal exposed (CoV)	Male	2W	15W	√		√	
P23	Maternal exposed (CoV)	Male	9W	17W	√		√	
P24	Uninfected (Ctrl)	Male	N/A	10W	√		√	
P25	Uninfected (Ctrl)	Male	N/A	12W	√		√	
P26	Uninfected (Ctrl)	Male	N/A	12W	√		√	
P27	Uninfected (Ctrl)	Male	N/A	11W		√		√
P28	Uninfected (Ctrl)	Male	N/A	11W		√		√
P29	Uninfected (Ctrl)	Female	N/A	13W		√		√

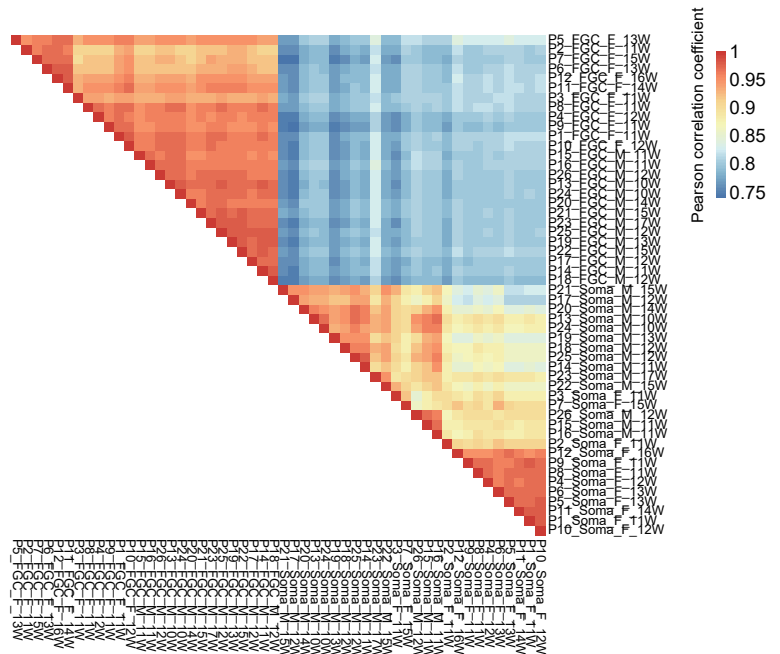D, day. W, week. N/A, not available.

B
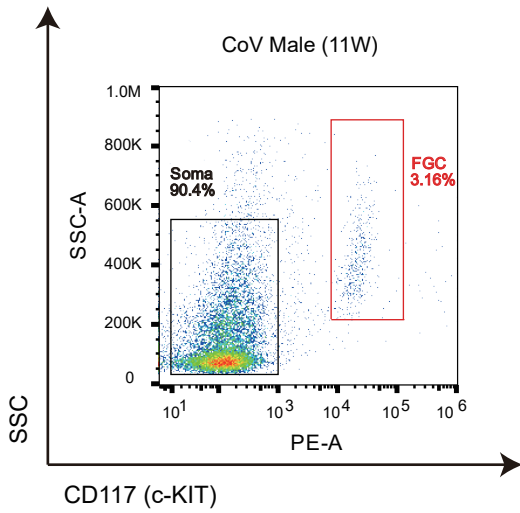
C

Figure S1

Figure S1. Isolation of human FGCs and gonadal somatic cells by FACS following maternal SARS-CoV-2 infection, related to Figure 1.

(A) Details of samples collected from developing fetuses for total RNA-seq or WGBS-seq. D, day. W, week. N/A, not available.

(B) Representative FACS images from one 11W male gonad following maternal infection. W, gestational week at termination.

(C) Heatmap showing Pearson correlation coefficients of all transcriptomes. F, female. M, male. W, gestational week at termination.
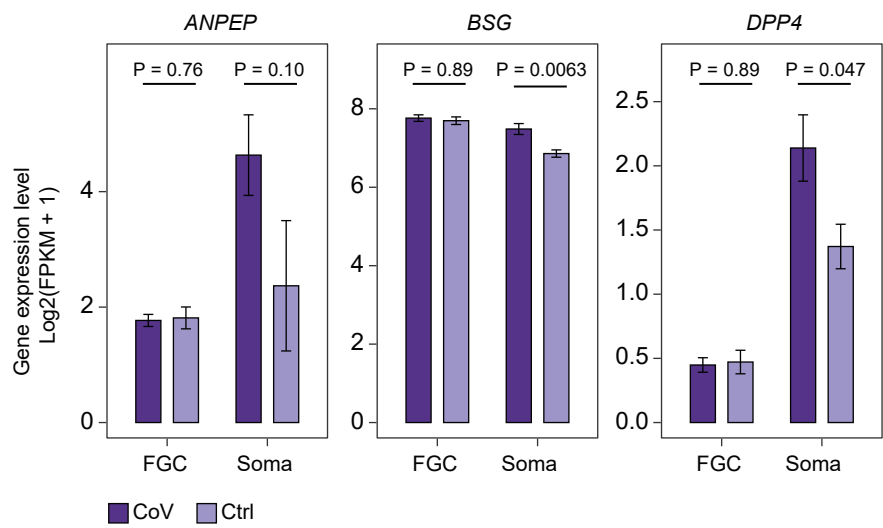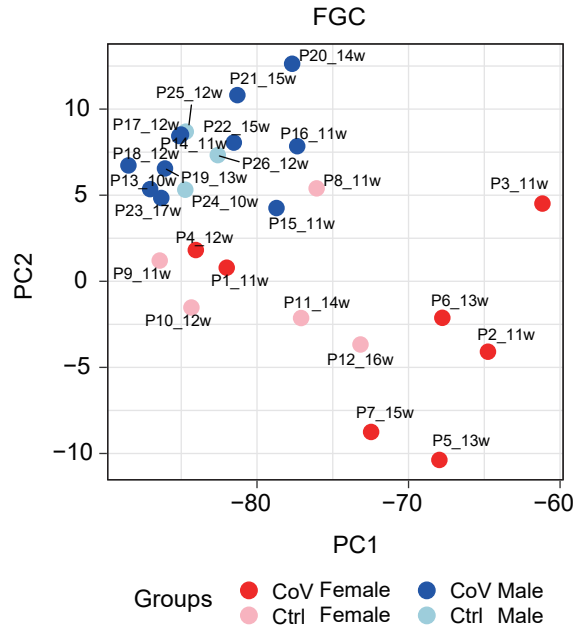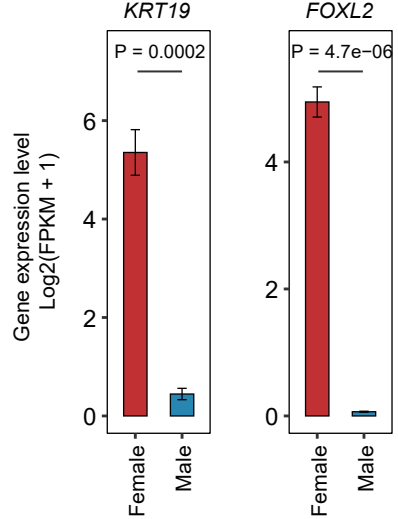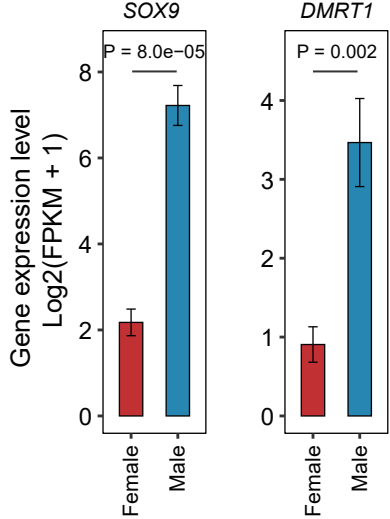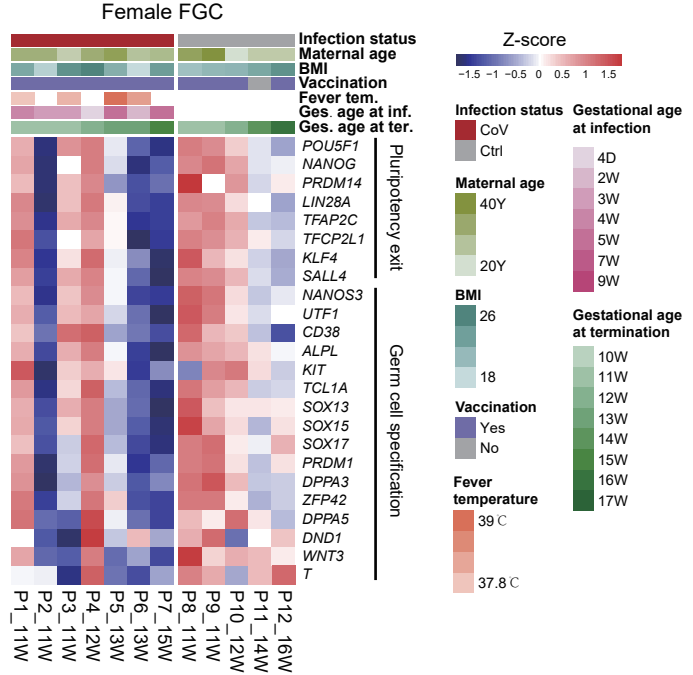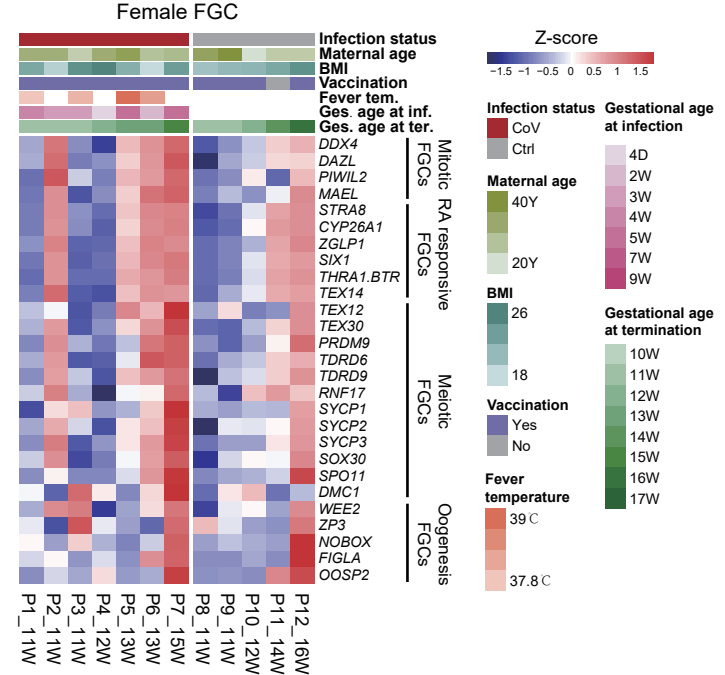
Figure S2

Figure S2. Expression pattern of human FGCs following maternal SARS-CoV-2 infection, related to Figure 2, 3.

(A) Expression level of selected SCARFs (SARS-CoV-2- and coronavirus-associated receptors and factors) in FGCs and gonadal somatic cells. The expression level was represented as log2(FPKM+1). P values were calculated by Wilcoxon rank sum test. CoV_n = 18, Ctrl_n = 8.

(B and C) Bar plots showing expression level of selected female (B) and male (C) gonadal somatic marker genes. The expression level was represented as log2(FPKM+1). The Student's *t*-test was performed to examine the statistical difference between female and male in Ctrl group. Red color scheme, female. Blue color scheme, male. Ctrl_Female_n = 5, Ctrl_Male_n = 3.

(D and E) Comparison of the expression level of early (D) or late (E) germline specific marker genes of female FGCs between CoV and Ctrl group. The expression level was Z-scored. The clinical characteristics of these samples were shown above correspondingly. Y, year. W, week. D, day. The heatmaps were ordered by gestational age at termination horizontally in each infection status.

(F) Principal component analysis (PCA) of the transcriptome of FGCs from CoV and Ctrl group. Red color scheme, female. Blue color scheme, male. W, gestational week at termination.
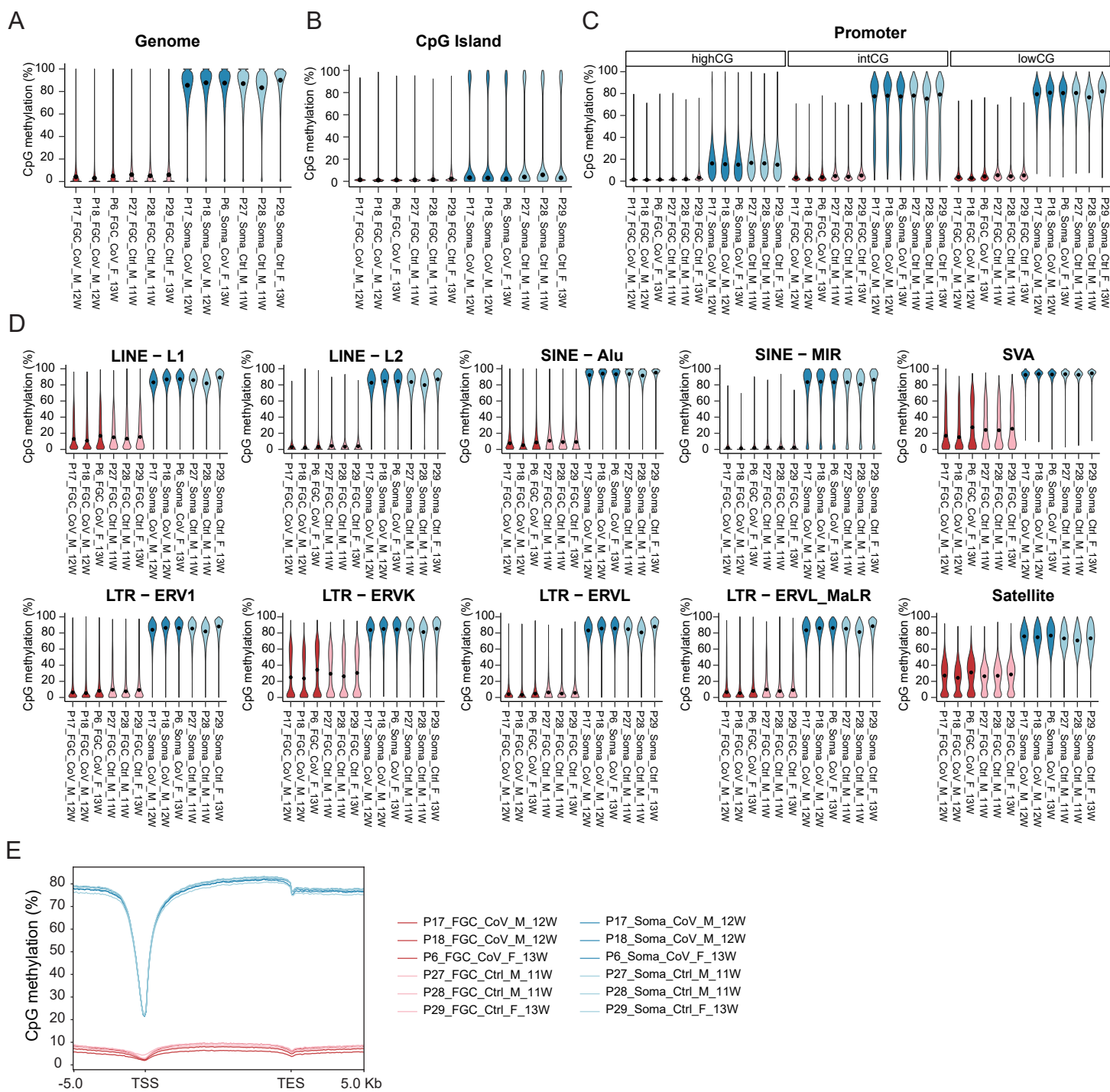
Figure S3

Figure S3. DNA methylation pattern of human FGCs and gonadal somatic cells following maternal SARS-CoV-2 infection, related to Figure 2, 3.

(A - D) Violin plots showing distribution of CpG methylation level in 500 bp sliding windows of whole genome (A), CpG Islands (B), promoter of genes (C), major human repetitive element classes and families (D) of FGCs and gonadal somatic cells from CoV and Ctrl group. F, female. M, male. W, gestational week at termination.

(E) Averaged CpG methylation level profiles of all genes from 5 Kb upstream (-) of transcription start sites (TSSs), through scaled gene bodies to 5 Kb downstream (+) of transcription end sites (TESs) in FGCs and gonadal somatic cells from CoV and Ctrl group. F, female. M, male. W, gestational week at termination.
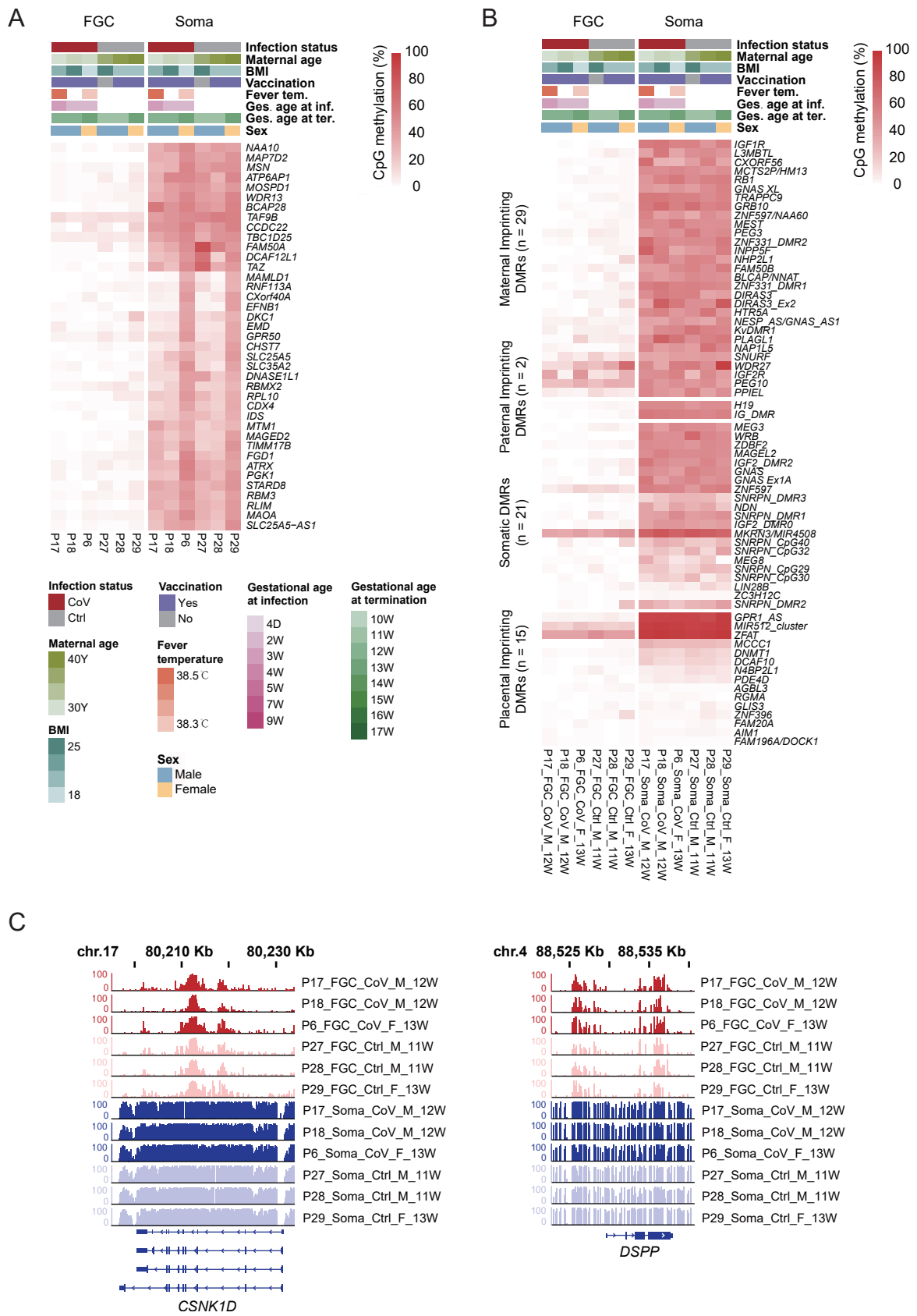
Figure S4

Figure S4. DNA methylation reprogramming faithfully maintained in human FGCs following maternal SARS-CoV-2 infection, related to Figure 3.

(A and B) DNA methylation dynamics of CGI-containing promoters on X chromosome (A) or imprinted differentially methylated regions (DMRs) (B) of FGCs and gonadal somatic cells from CoV and Ctrl group. The clinical characteristics of these samples were shown above correspondingly. Y, year. W, week. D, day. The heatmaps were ordered by gestational age at termination horizontally in each infection status.

(C) IGV plots showing the DNA methylation level profiles of two representative regions that evaded genome-wide DNA demethylation in FGCs ("escapees"). F, female. M, male. W, gestational week at termination.
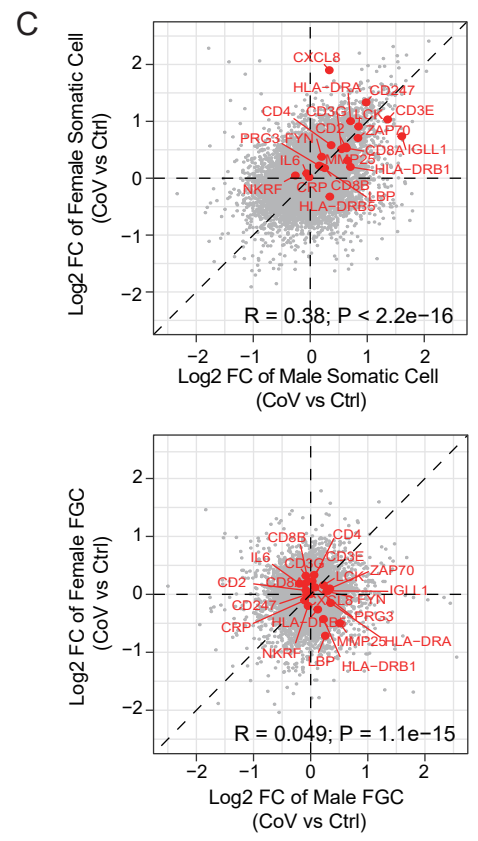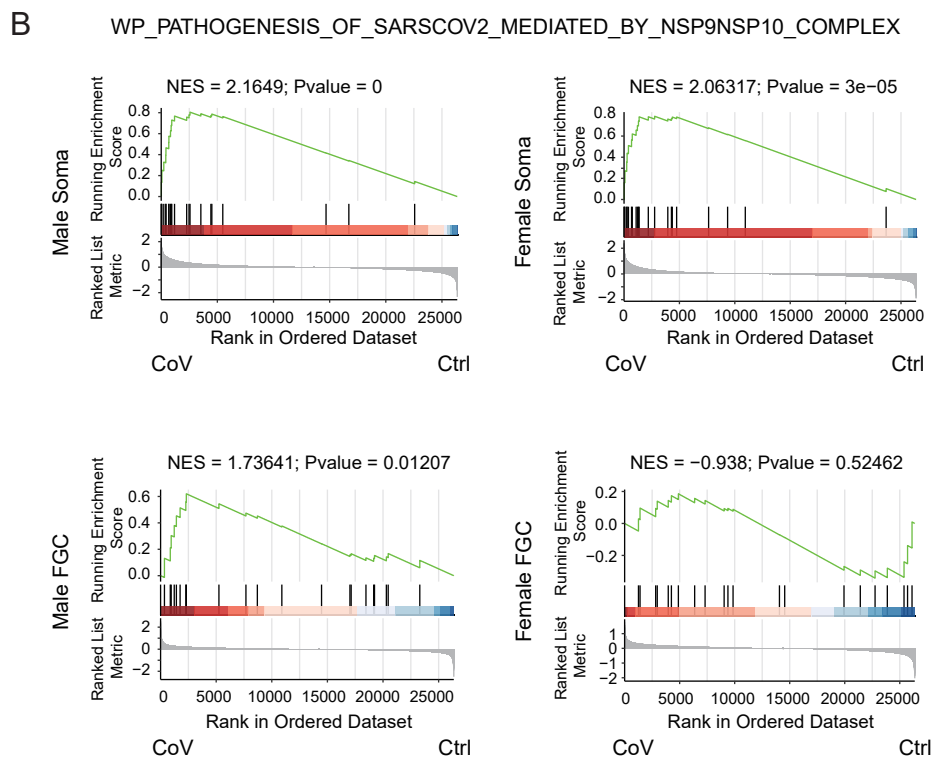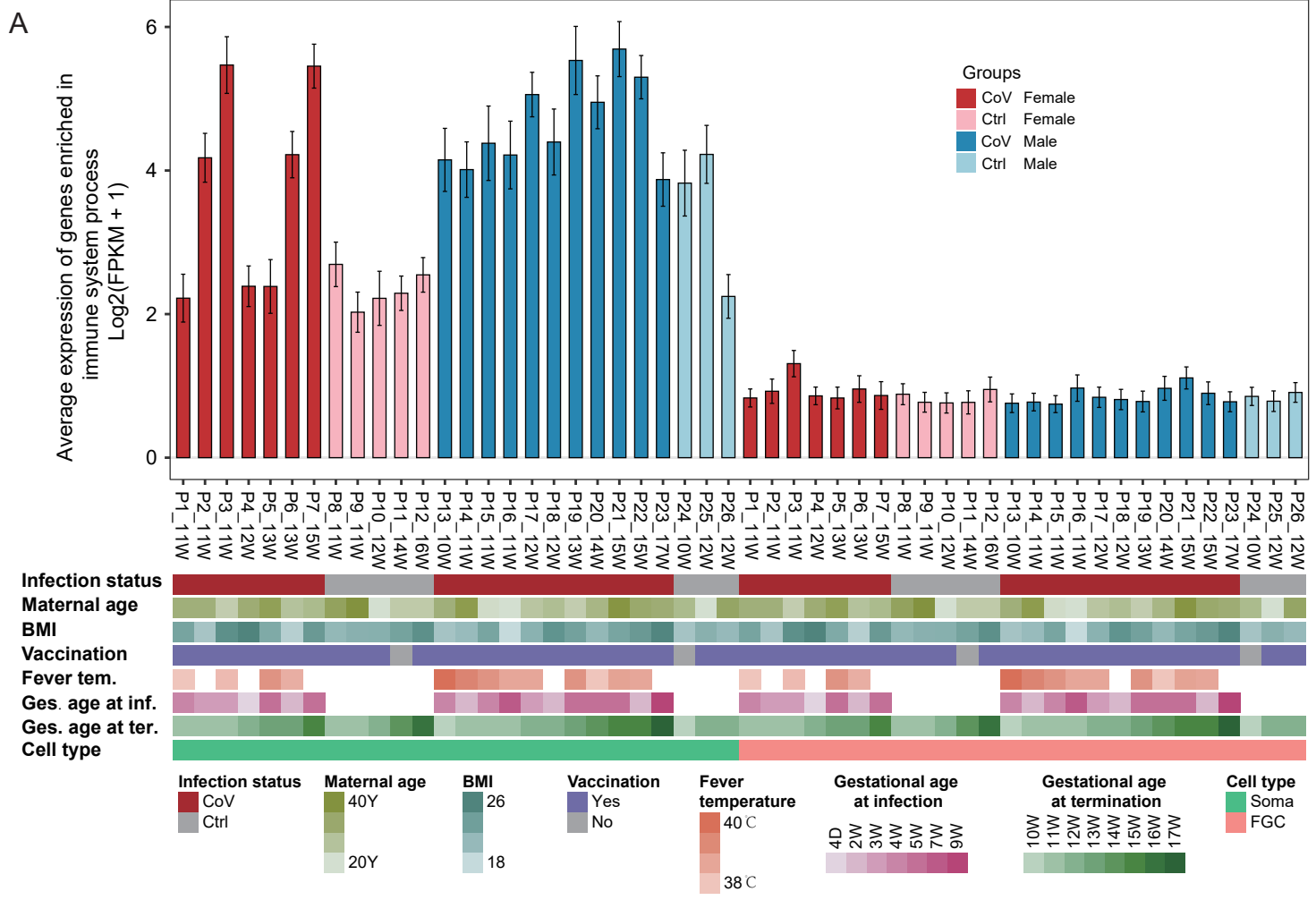
Figure S5

Figure S5. Extensive immune responses in gonadal niche shield FGCs from maternal SARS-CoV-2 infection, related to Figure 4.

(A) The average expression level of co-upregulated genes in both male and female gonadal somatic cells and FGCs, which enriched in the top GO term "immune system process". The clinical characteristics of these samples were shown below correspondingly. Y, year. W, week. D, day. The bar plot was ordered by gestational age at termination horizontally in each group.

(B) The selected top enriched pathway of Figure 4G was shown by GSEA enrichment plot in male and female gonadal somatic cells and FGCs, respectively. The NES and P value were shown. NES, normalized enrichment score.

(C) Scatter plots showing the alternations of gene expression of all genes calculated by CoV group versus Ctrl group in male and female gonadal somatic cells (C, top) and FGCs (C, bottom), respectively. The alternation of gene expression was represented as log2 fold change (log2 FC). The representative genes related to the pathways shown in (B) were labeled in red. The Pearson correlation coefficients and the P values were shown. CoV_Male_n = 11, Ctrl_Male_n = 3, CoV_Female_n = 7, Ctrl_Female_n = 5.
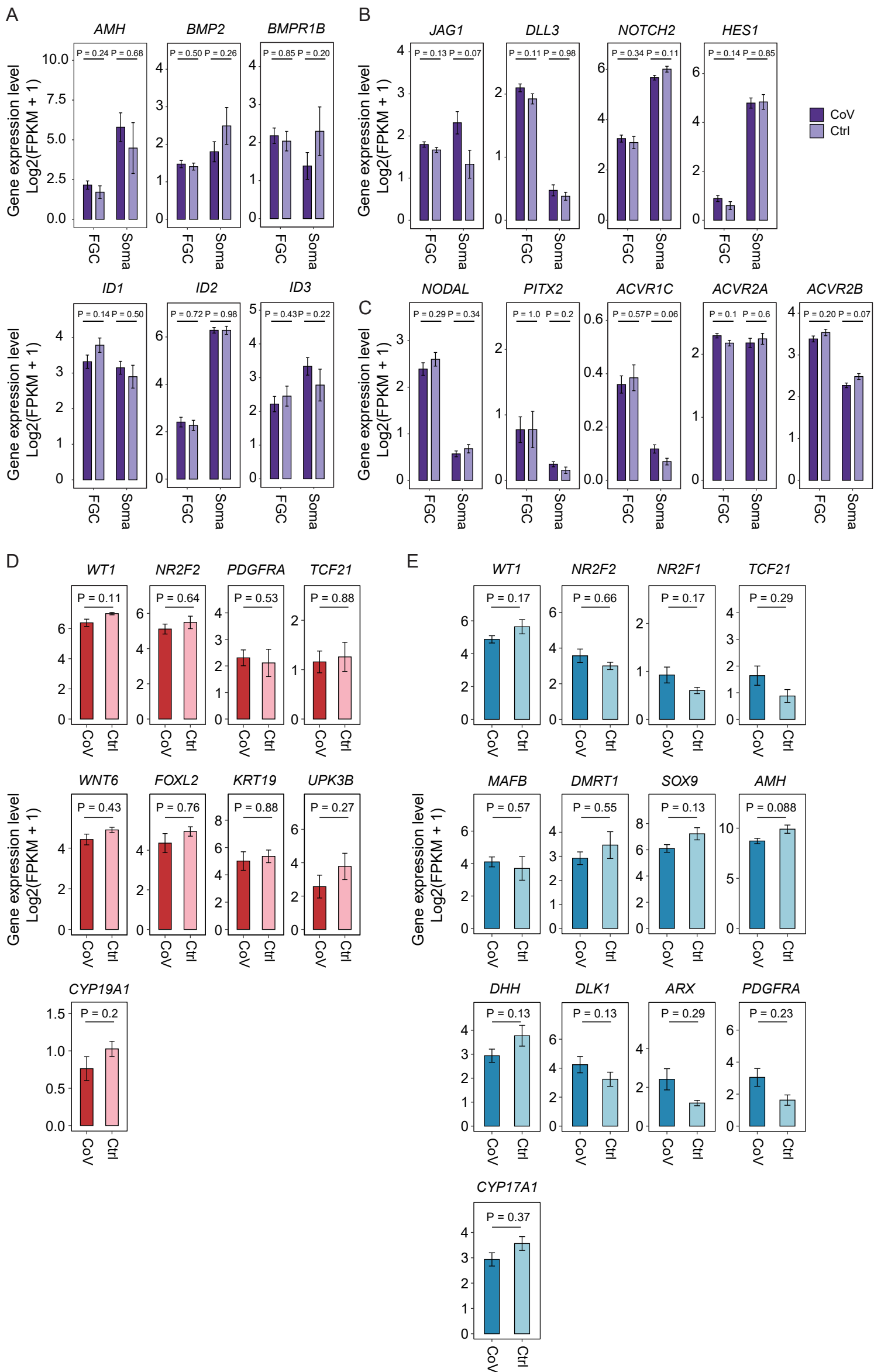
Figure S6

Figure S6. Human FGC-niche communication was not compromised following maternal SARS-CoV-2 infection, related to Figure 4.

(A - C) Bar plots showing expression level of the specific ligands, receptors, and target genes of the BMP (A), NOTCH (B) and NODAL (C) signaling pathways. The expression level was represented as log2(FPKM+1). P values were calculated by Wilcoxon rank sum test. CoV_n = 18, Ctrl_n = 8.

(D and E) Bar plots showing expression level of selected female (D) and male (E) gonadal somatic marker genes. The expression level was represented as log2(FPKM+1). The Student's *t*-test was performed to examine the statistical difference between the CoV group and Ctrl group. Red color scheme, female. Blue color scheme, male. CoV_Female_n = 7, Ctrl_Female_n = 5, CoV_Male_n = 11, Ctrl_Male_n = 3.